Distribution Agreement

In presenting this thesis as a partial fulfillment of the requirements for a degree from Emory University, I hereby grant to Emory University and its agents the non-exclusive license to archive, make accessible, and display my thesis in whole or in part in all forms of media, now or hereafter now, including display on the World Wide Web. I understand that I may select some access restrictions as part of the online submission of this thesis. I retain all ownership rights to the copyright of the thesis. I also retain the right to use in future works (such as articles or books) all or part of this thesis.

Julia Gensheimer April 9, 2019

Differentiation pathway of virus-specific stem-like $CD8^+$ T cells during chronic infection

by

Julia Gensheimer

Rafi Ahmed
Adviser

Department of Biology

Rafi Ahmed

Adviser

Haydn Kissick

Committee Member

Arri Eisen

Committee Member

2019

Differentiation pathway of virus-specific stem-like $CD8^+$ T cells during chronic infection

by

Julia Gensheimer

Rafi Ahmed

Adviser

An abstract of
a thesis submitted to the Faculty of Emory College of Arts and Sciences
of Emory University in partial fulfillment
of the requirements of the degree of
Bachelor of Sciences with Honors

Biology

2019

Abstract

Differentiation pathway of virus-specific stem-like $CD8^+$ T cells during chronic infection

By Julia Gensheimer

T cell exhaustion is a characteristic feature of chronic viral infection and cancer. Exhausted $CD8^+$ T cells are marked by the expression of negative regulatory surface proteins and progressive loss of effector function. Targeting checkpoint molecules expressed on exhausted $CD8^+$ T cells restores their proliferative capacity, cytotoxicity, and cytokine production. These molecules, such as PD-1 pathway inhibitors, are successful at treating many cancer types; however, not all tumor types are susceptible nor do all patients with these tumors respond. Two major obstacles to improving immunotherapy are the co-expression of multiple inhibitory proteins on the surface of exhausted $CD8^+$ T cells and the heterogeneity present within the antigen-specific $CD8^+$ T cell pool in chronic viral infection and cancer. In the mouse lymphocytic choriomeningitis virus model of chronic infection, two antigen-specific $CD8^+$ T cell populations have been identified: a PD-1^+ Tcf-1^+ stem-like subset capable of self-renewal and differentiation into a second, more terminally-differentiated PD-1^+ $Tim3^+$ effector-like population. These Tcf-1^+ stem-like $CD8^+$ T cells have now been found in a variety of chronic viral infections and human tumors. Here, we perform RNA-sequencing to comprehensively identify the repertoire of cell surface molecules expressed by these two exhausted $CD8^+$ T cell populations. We find that expression of CD101 divides PD-1^+ $Tim3^+$ $CD8^+$ T cells into two distinct populations. Using adoptive transfer experiments, we show that the stem-like Tcf-1^+ $CD8^+$ T cells initially differentiate into a transitory population of $CD101^-$ $Tim3^+$ cells that later irreversibly convert into $CD101^+$ $Tim3^+$ cells. $CD101^+$ $Tim3^+$ $CD8^+$ T cells are transcriptionally distinct from both stem-like and $CD101^-$ $Tim3^+$ transitory cells, including altered expression of transcription factors and high levels of many checkpoint molecules. In contrast, recently-generated $CD101^-$ $Tim3^+$ cells show a distinct, effector-like transcriptional signature and are more functional than the terminally differentiated $CD101^+$ $Tim3^+$cells. PD-1 pathway blockade increases the numbers of these newly-generated $CD101^-$ $Tim3^+$ $CD8^+$ T cells, suggesting that these transitory and more functional cells may play a critical role in PD-1 based immunotherapy.

Differentiation pathway of virus-specific stem-like $CD8^+$ T cells during chronic infection

by

Julia Gensheimer

Rafi Ahmed

Adviser

A thesis submitted to the Faculty of Emory College of Arts and Sciences
of Emory University in partial fulfillment
of the requirements of the degree of
Bachelor of Sciences with Honors

Biology

2019

Acknowledgements

The authors would like to thank postdoctoral fellow, Dr. William Hudson, for his pivotal contributions to the following thesis. Will is a Cancer Research Institute Irvington Fellow supported by the Cancer Research Institute. We would also like to acknowledge the following members of the Ahmed lab for their support: Masao Hashimoto, Andreas Wieland, Rajesh M. Valanparambil, Bogumila T. Konieczny, and Se Jin Im. We also appreciate the contributions of Haydn T. Kissick in the Department of Urology. Haydn is supported by grant K99CA197804 from the National Cancer Institute of the National Institutes of Health (NIH). In addition, the authors thank Robert Karaffa and Kametha Fife of the Emory University School of Medicine Flow Cytometry Core and Alice Kamphorst, Koichi Araki, and Timothy Hoang. Julia Gensheimer is supported by Emory Undergraduate Research programs. Rafi Ahmed is supported by grant R01AI030048 from the National Institute of Allergy and Infectious Diseases of the NIH. The Yerkes Nonhuman Primate Genomics Core is supported in part by ORIP/OD P51OD011132.

Table of Contents

Introduction

Since the early 2000s, immunotherapy has revolutionized the medical field with its unique approach to treating cancer and other diseases (Pardoll, 2011). What distinguishes immunotherapy from other targeted therapies is the manipulation of host immune cells to restore their native disease-fighting abilities. $CD8^+$, or cytotoxic, T cells are key players in this treatment. Generated in the thymus, $CD8^+$ T cells patrol the body in search of pathogen-infected cells (Zhang et al., 2011). Upon recognition of its respective antigen, a naive $CD8^+$ T cell differentiates into an effector state, which is marked by high proliferation and cytotoxic capability. These cells attack and kill infected host cells expressing intracellular non-self or mutated-self antigens arising from infection or cell transformation. After clearance of an acute viral infection, memory precursor cells present in the heterogenous pool of effector $CD8^+$ T cells will differentiate into long-lived memory cells in the absence of antigen (Joshi et al., 2007; Sarkar et al., 2008). These memory cells remain primed for rapid effector responses upon antigen re-exposure, providing protective immunity against re-infection (Akondy et al., 2017; Kaech et al., 2002).

In conditions marked by persistent antigen like cancer or chronic viral infection, $CD8^+$ T cells enter an 'exhausted' state. These cells express regulatory surface proteins such as PD-1 (Day et al., 2006) and progressively lose their proliferative capacity, cytotoxicity, and cytokine production (Zajac et al., 1998; Moskophidis et al., 1993). To combat exhaustion, antibodies known as immune checkpoint inhibitors target negative regulatory surface proteins on exhausted $CD8^+$ T cells, restoring effector functions (Callahan and Wolchok, 2013). These drugs, such as PD-1 pathway inhibitors, are successful at treating many cancer types; however, not all tumor types

are susceptible nor do all patients with these tumors respond (Topalian et al., 2012; Brahmer et al., 2012). This resistance to certain checkpoint inhibitors has inspired the search for other inhibitory surface molecules expressed on $CD8^+$ T cells for use as immunotherapy targets, often for use in combination with anti-PD-1 pathway blockade (Pardoll, 2012; Ott et al., 2017).

Another factor that complicates PD-1 therapy is the heterogeneity in exhausted $CD8^+$ T cell populations. A recent study identified the presence of a 'stem-like' population of PD-1^+Tcf-1^+ $CXCR5^+CD8^+$ T cells that sustain $CD8^+$ T cell responses during chronic viral infection and give rise to PD-1^+Tim3^+ terminally differentiated cytotoxic cells (Im et al., 2016; Utzschneider et al., 2016; Wu et al., 2016). Stem-like $CD8^+$ T cells are found in numerous types of chronic infections and human cancers (Brummelman et al., 2018; Gettinger et al., 2018; He et al., 2016; Jiang et al., 2017; Leong et al., 2016), and it is these Tcf-1^+ stem-like cells that mediate the proliferative response to PD-1 pathway blockade (Im et al., 2016). In contrast, PD-1^+Tim3^+ cells do not undergo significant amounts of division after PD-1 blockade (Im et al., 2016). This heterogeneity again highlights the need for identification of additional surface markers of PD-1 responsive cells and targets for combination therapy to bring additional antigen-specific $CD8^+$ T cells into the immunotherapy-responsive pool.

Here, we perform a systematic approach to catalog the repertoire of surface molecules expressed by exhausted $CD8^+$ T cells. We analyzed RNA-sequencing data obtained from antigen-specific $CD8^+$ T cells of mice infected with lymphocytic choriomeningitis virus (LCMV) strains Armstrong or clone 13, which cause an acute or chronic infection respectively. LCMV is a natural rodent infection commonly used in immunological studies (Zhou et.al, 2012). Its use as a model

pathogen has led to the discovery of key concepts in immunology, such as T cell exhaustion and memory generation.

From this analysis we identified molecules specifically upregulated on exhausted cells compared to naive, effector, and memory $CD8^+$ T cells. We confirmed well-known markers of exhaustion such as PD-1, Tim3, and CD244 (2B4), but also identified other novel surface molecules with less-studied roles in T cell exhaustion such as CD7, Lax1, CD200R, and CD101. Due to their unique phenotypes, we chose to examine cells expressing the latter molecule in the following thesis. While the protein structure and binding interactions of CD101 are unknown, previous studies describe it as a marker of dysfunctional cells (Zhang et al., 2019; Philip et al., 2017). Most notably, $CD101^+CD38^+PD1^+CD8^+$ T cells and tumor infiltrating lymphocytes (TILs) were unresponsive to PD-1 blockade and a predictor of poor survival for pancreatic cancer patients (Zhang et al., 2019).

In the following thesis, we demonstrate that CD101 is induced specifically on $CD8^+$ T cells in chronic viral infection and that its expression marks terminally differentiated and highly dysfunctional antigen-specific $CD8^+$ T cells. Further, we show that stem-like $CD8^+$ T cells differentiate into transitory $CD101^-Tim3^+$ cells that retain substantial proliferative and effector capacity before eventual progression into an exhausted $CD101^+Tim3^+$ state. Finally, we show that PD-1 pathway blockade leads to greater numbers of transitory antigen-specific $CD101^-Tim3^+$ cells, demonstrating that PD-1 pathway blockade increases both the quality and quantity of antigen-specific $CD8^+$ T cells.

Methods

Identifying novel markers of murine CD8$^+$ T cell exhaustion

To identify gene expression patterns on exhausted CD8$^+$ T cells, we sequenced RNA from cells of mice infected with LCMV Armstrong or clone 13. This RNA-sequencing data from acute and chronic LCMV infection were previously described (Hudson et al., 2019). For subsets from chronic infection, tetramer-positive CXCR5$^+$Tim3$^-$ and CXCR5$^-$Tim3$^+$ LCMV-specific cells were isolated by fluorescence activated cell sorting (FACS) from spleens of mice infected with LCMV clone 13, infected as described below. For both datasets, reads were aligned to the mm10 genome (accessed through *Ensembl* (Zerbino et al., 2018)) with HISAT2 version 2.0.5 (Kim et al., 2015). featureCounts (Liao et al., 2013) was used to assign aligned reads to genes using the *Ensembl* release 91 mouse genome annotation, with reads overlapping multiple features allowed assignment to more than one gene. To control for batch effects, counts were normalized with DESeq2 (Love et al., 2014) with a design formula of ~type+batch, where 'type' indicates the cell type (Naive, Memory Precursor, CXCR5$^+$, etc.) and 'batch' indicates the individual RNA-seq experiment (acute and chronic LCMV infection).

To identify transmembrane proteins, all peptide sequences (including splice variants) for all protein-coding genes in the *Ensembl* 91 genome annotation were accessed through the biomaRt R package (Durinck et al., 2005; Durinck et al., 2009) and transmembrane helices predicted by the TMHMM server version 2.0 (Krogh et al., 2001). To identify ITAM, ITIM, and ITSM motifs, predicted intracellular regions were scanned for the motifs Yxx(I/L)x_{6-8}(Y)xx(I/L), (I/L/S/V)xYxx(I/L/V), and TxYxx(A/L/V), respectively, using a custom Python script. Genes were labeled as transmembrane if *any* of its annotated protein sequence contained a predicted

transmembrane helix, and genes were labeled as containing an ITAM, ITIM, or ITSM if *any* of its annotated protein sequences had the appropriate motif within a predicted intracellular region. Genes were identified as containing an immunoglobulin-like domain if the gene was annotated as containing at least one of the following PFAM domains (Finn et al., 2016) as accessed through biomaRt (Durinck et al., 2005; Durinck et al., 2009): PF00047, PF02124, PF02440, PF02480, PF03921, PF06697, PF07654, PF07679, PF07686, PF08204 PF08205, PF11465, PF13895, PF13927, PF15028, PF16680, PF16681, or PF16706.

A gene was identified as a marker of $Tim3^+$ $CD8^+$ T cells from LCMV clone 13 infection if the gene met *all* of the following conditions:

1. Expression > 1000 normalized counts in $Tim3^+$ $CD8^+$ T cells
2. Expression in $CXCR5^-Tim3^+$ $CD8^+$ T cells > expression in $CXCR5^+Tim3^-$ $CD8^+$ T cells
3. $\log_2$ fold change ($CXCR5^-Tim3^+$ $CD8^+$ T cells / naive $CD8^+$ T cells) > 1.6 (~ 3-fold)
4. $\log_2$ fold change ($CXCR5^-Tim3^+$ $CD8^+$ T cells / terminal effector $CD8^+$ T cells) > 1.6
5. $\log_2$ fold change ($CXCR5^-Tim3^+$ $CD8^+$ T cells / effector memory $CD8^+$ T cells) > 1.6

A gene was identified as a marker of $CXCR5^+$ $CD8^+$ T cells from LCMV clone 13 infection if the gene met *all* of the following conditions:

1. Expression > 1000 normalized counts in CXCR5+ $CD8^+$ T cells
2. Expression in $CXCR5^+Tim3^-$ $CD8^+$ T cells > expression in $CXCR5^-Tim3^+$ $CD8^+$ T cells
3. $\log_2$ fold change ($CXCR5^+Tim3^-$ $CD8^+$ T cells / naive $CD8^+$ T cells) > 1.6
4. $\log_2$ fold change ($CXCR5^+Tim3^-$ $CD8^+$ T cells / terminal effector $CD8^+$ T cells) > 1.6
5. $\log_2$ fold change ($CXCR5^+Tim3^-$ $CD8^+$ T cells / effector memory $CD8^+$ T cells) > 1.6

As gene expression changes can become dampened with higher expression, the required $\log_2$ fold change in conditions 3-5 above were relaxed to 1.0 (2-fold) for genes with expression >7500 normalized counts.

RNA-sequencing and analysis of CD101 subsets from chronic LCMV infection

$CD101^-Tim3^-$, $CD101^-Tim3^+$, and $CD101^+Tim3^+$ $PD\text{-}1^+CD8^+$ T cells were isolated by FACS from three pools of ten mice each infected with LCMV clone 13 >45 days prior to the sort. Separately, naive $CD8^+$ T cells from three age-matched uninfected mice were also isolated by FACS. RNA was isolated using the Qiagen AllPrep Micro kit according to the manufacturer's protocols. RNA sequencing with poly(A) selection was performed at the Yerkes Nonhuman Primate Genomics Core.

As above, reads were aligned with HISAT2 version 2.0.5 (Kim et al., 2015) to the mm10 genome (accessed through *Ensembl* (Zerbino et al., 2018)) and featureCounts (Liao et al., 2013) was used to assign aligned reads to genes using the *Ensembl* release 91 mouse genome annotation. DESeq2 (ref. (Love et al., 2014)) was used to normalize for library size and calculate differential expression across groups. A gene was considered differentially expressed between two groups with an adjusted p-value of <0.05 and an average expression of >20 normalized counts across all samples.

For gene set enrichment analysis, GSEA preranked (Subramanian et al., 2005) was used against the MSigDB (Liberzon et al., 2015; Liberzon et al., 2011), with $-\log_{10}(p) * \text{sign}(\log_2(FC))$ as the ranking statistic, where p is the adjusted p-value and FC the fold change of the differential expression analysis of interest. Enrichment was considered significant with an FDR < 0.05.

Principal component analysis was performed with the factomineR R package(Lê et al., 2008) on all detected genes using the regularized log transformation from DESeq2. One sample of $CD101^{-}Tim3^{-}$ cells was excluded from dimensionality reduction due to its status as an outlier on PCA but included on all other analyses. RNA-sequencing data was visualized with the ggplot2 R package (Wickham, 2016) and GraphPad Prism (version 7.0c). RNA-sequencing reads are available from the NCBI Sequence Read Archive under accession PRJNA497086.

Mouse infection experiments

LCMV infections were performed as previously described (Araki et al., 2017; Im et al., 2016). For chronic infections, 6-8 week old C57BL/6JB6 (B6) mice were injected intraperitoneally (i.p.) with 300 μg of CD4-depleting antibody GK1.5 (Bio X Cell) one and two days before intravenous (i.v.) injection with 2×10^6 pfu LCMV clone 13. This infection when coupled with $CD4^+$ T cell depletion lasts the lifetime of the mouse. For acute infection, B6 mice were injected i.p. with 2×10^5 pfu LCMV Armstrong. Unless otherwise indicated, LCMV Armstrong-infected mice were analyzed at day 8 post-infection for the acute timepoint and after day 45 for the memory timepoint. Unless otherwise indicated, LCMV clone 13-infected mice were analyzed after day 45 for the chronic timepoint.

B6 mice were obtained from The Jackson Laboratory. P14 mice, with transgenic T cell receptors (TCRs) specific to LCMV, were bred in-house. P14 cells create a well-controlled experiment as every donor T cell will respond to the LCMV infection within the context of infection of the same mouse. All mouse experiments were performed with approval of the Emory University Institutional Animal Care and Use Committee.

Adoptive transfer experiments

Splenocytes were isolated from LCMV clone 13 infected B6 mice >45 days after infection. $CD8^+$ T cells were separated with the EasySep Mouse $CD8^+$ T Cell Isolation Kit (StemCell) and subsequently labeled with CellTrace Violet (CTV, ThermoFisher) according to the manufacturer's protocol. Using FACS, three populations of PD-1^+CD8^+ T cells were isolated ($CD101^-Tim3^-$, $CD101^-Tim3^+$, $CD101^+Tim3^+$). Cells were reconstituted in RPMI and 9-10 x 10^4 isolated cells from a single population were transferred i.v. to recipient $CD45.1^+$ B6 mice. Two weeks after transfer, cells were isolated from spleen, liver, lung, and bone marrow and stained as below.

Intracellular cytokine staining experiments

2 x 10^3 P14 cells (cells with a transgenic TCR for the D_b-restricted gp33 LCMV epitope) were transferred i.v. to recipient mice three days before infection with LCMV clone 13 as described above. Twenty-two days after infection, splenocytes were isolated and incubated in RPMI with 10% FBS with 0.2 µg/ml of gp33 peptide for five hours at 37 °C in the presence of BD GolgiStop and BD GolgiPlug, according to manufacturer's protocols. After incubation, cells were stained for flow cytometry as described below.

PD-L1 blockade experiments

Mice were infected as above with LCMV clone 13. >45 days after infection, mice were injected with 200 µg of αPD-L1 (clone 29F.1A12) in phosphate buffered saline (PBS) or an equivalent volume of PBS alone. Injections were given i.p. every three days. Mice were analyzed for responses 12 or 14 days after initiation of treatment.

Flow cytometry experiments

MHC I tetramers were prepared and used as previously described (Murali-Krishna et al., 1998). Single cell suspensions were stained with antibodies and/or tetramer in PBS with 2% fetal bovine serum (FBS) and 2 mM EDTA for extracellular targets. For intranuclear staining, the eBioscience Foxp3 / Transcription Factor Staining Buffer Set was used for fixation, permeabilization, and intracellular staining. BD Cytofix/Cytoperm and Perm/Wash buffers were used for fixation and staining of cytoplasmic targets. BD Cytofix/Cytoperm was also used for fixation of non-intracellularly stained cells. Samples were acquired using a BD LSR II and analyzed using FlowJo. Summary graphs and statistics were performed in GraphPad Prism v7.

Results

Systematic identification of CD8$^+$ T cell exhaustion markers

We analyzed two RNA-sequencing datasets generated by our laboratory to identify murine markers of CD8$^+$ T cell exhaustion (**Figure 1a**). The first dataset describes RNA-sequencing data from virus-specific CD8$^+$ T cells from the spleens of mice infected with LCMV Armstrong, which causes an acute infection that results in both functional effector and memory CD8$^+$ T cell responses (Hudson et al, 2019). At the peak of the CD8$^+$ T cell response to LCMV Armstrong, a heterogeneous effector cell pool is present, including Klrg1^{hi}CD127^{lo} terminal effector cells (TEs) and Klrg1^{lo}CD127^{hi} memory precursor cells (MPs) (Joshi et al., 2007; Kaech et al., 2003). While both populations produce cytokines and exhibit cytotoxicity, the CD127$^+$ MPs differentiate into long-lived memory CD8$^+$ T cells (Kaech et al., 2003; Sarker et al., 2008). To generate this first dataset, LCMV-specific MPs and TEs were isolated by fluorescence-activated cell sorting (FACS) eight days after infection. Forty-eight days post-infection, CD127$^+$CD62L$^+$ central memory cells (CM) and CD127$^+$CD62L$^-$ effector memory (EM) LCMV-specific cells were isolated by FACS (Sallusto et al., 1999; Wherry et al., 2003). RNA from these subsets and naive cells was isolated from sorted cells and sequenced.

The second dataset consist of RNA-sequencing data of LCMV-specific CD8$^+$ T cells present in chronic infection caused by LCMV clone 13. Two cell populations, PD-1$^+$CXCR5$^+$Tim3$^-$ cells and PD-1$^+$CXCR5$^-$Tim3$^+$ cells, were isolated from spleens of mice infected with LCMV clone 13. The first subset is a stem-like population of cells that express Tcf-1 and have the capability for self-renewal. The latter subset (Tim3$^+$) is a terminally-differentiated CD8$^+$ T cell population that does not proliferate in response to PD-1 blockade (Im et al., 2016). In both studies, naive CD8$^+$ T cells

were sequenced to compare $CD8^+$ T cells from uninfected mice and act as a control population between the two studies.

To identify surface proteins upregulated in exhausted $CD8^+$ T cells, we selected genes with both high absolute expression and high relative expression (>3 fold) compared to naive, TE, and EM $CD8^+$ T cells (**Figure 1b**). Because of the vast amount of data received by RNA-sequencing, we narrowed down our list of candidate genes by looking only at those encoding surface proteins. These genes were distinguished by the presence of a predicted transmembrane helix (Krogh et al., 2001) in their associated peptide sequences (**Figure 1c**). In addition, immunoreceptor tyrosine-based motifs were determined in predicted intracellular regions and proteins with immunoglobulin (Ig)-like domains were identified via PFAM annotations (Finn et al., 2016) (**Figure 1c**). These Ig-like domains are often important for protein-protein interactions in immunological signaling pathways (Barclay, 2003).

In total, we identified 49 transmembrane proteins significantly upregulated in PD-1^+Tim3^+ LCMV-specific $CD8^+$ T cells from chronically infected mice (**Figure 1d**). This included several well-known inhibitory coregulatory molecules, such as PD-1 (*Pdcd1*), Lag3, and 2B4 (*Cd244*). Our analysis also identified several encoding proteins with described negative effects on T cell receptor (TCR) signaling but poorly understood roles in $CD8^+$ T cell exhaustion, such as *Lax1*, *Cd101*, and *Pvrig*, which encodes an inhibitory receptor for CD112 (Philip et al., 2017; Soares et al., 1998; Zhu et al., 2016). An additional 20 genes encoding transmembrane proteins were identified as highly and selectively expressed in the stem-like $CXCR5^+CD8^+$ T cells from chronic LCMV infection (Im et al., 2016). These include *Slamf6*, a putative stimulatory molecule

(Chatterjee et al., 2011), and several molecules typically expressed on B cells or CD4⁺ T cells, such as *Cd22* and *Cxcr5* (**Figure 1e**).

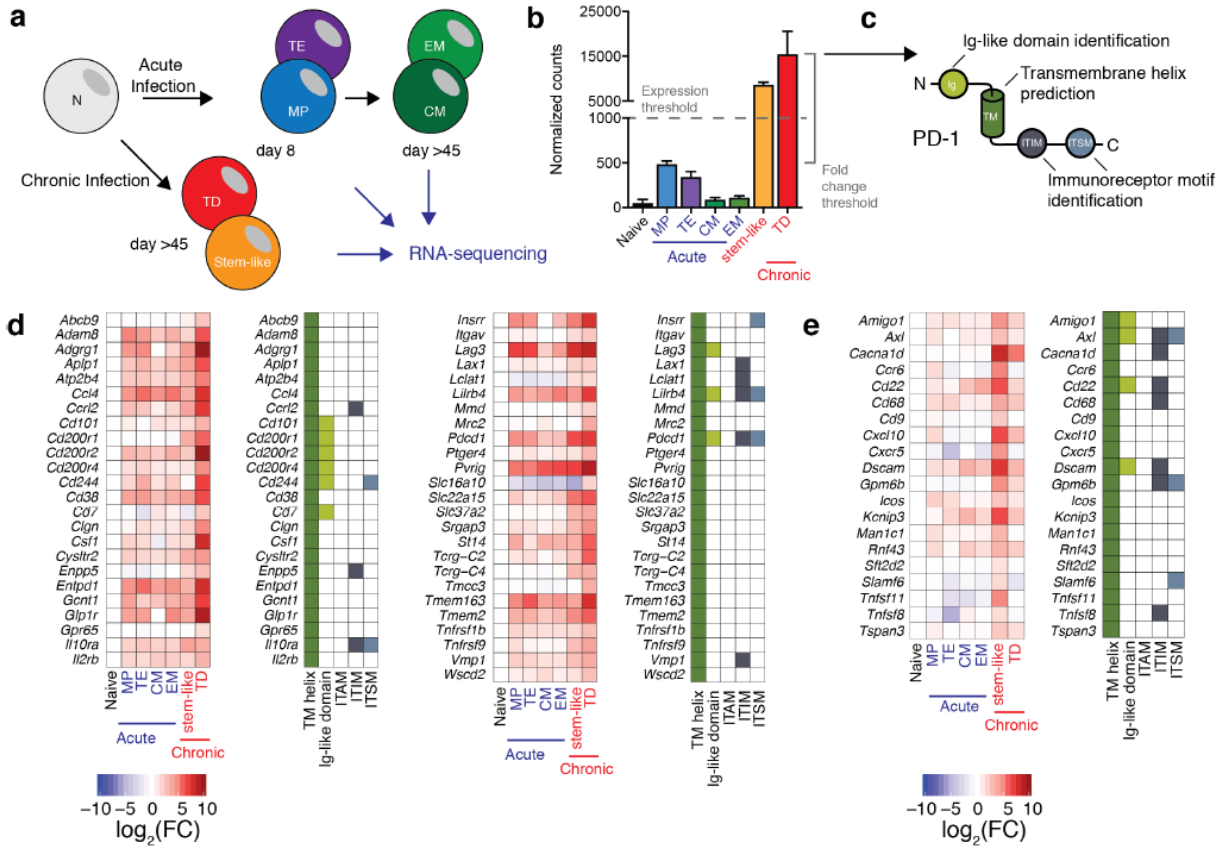

Figure 1: Systematic identification of CD8⁺ T cell exhaustion markers.

a) Naive and virus-specific CD8⁺ T cells from acute and chronic LCMV infection were isolated and analyzed for gene expression by RNA-sequencing. b) After analysis, genes with high absolute expression in exhausted CD8⁺ T cells from chronic infection and high relative expression compared to naive CD8⁺ T cells and cells from acute infection were identified. c) A bioinformatics pipeline to identify transmembrane helices, putative intracellular signaling motifs, and immunoglobulin-like domains was performed on identified genes. PD-1, the gene product of *Pdcd1*, is shown as an example. d) Heatmap of expression and protein properties of the 49 transmembrane helix-containing genes identified as highly expressed in Tim3⁺ CD8⁺ T cells from chronic infection by this algorithm. At left, $\log_2$ of the fold change from naive cells is shown. e) Heatmap of expression and protein properties of the 20 transmembrane helix-containing genes identified as highly expressed in stem-like CD8⁺ T cells from chronic infection.

To confirm the genes above as markers of exhausted CD8⁺ T cells, we performed flow cytometry to examine protein expression of selected markers on the surface of CD8⁺ T cells from uninfected mice, mice infected with LCMV Armstrong at acute and memory time points, and mice infected chronically with LCMV clone 13 (**Figure 2**). In all cases, expression of identified markers was consistent with RNA-sequencing data.

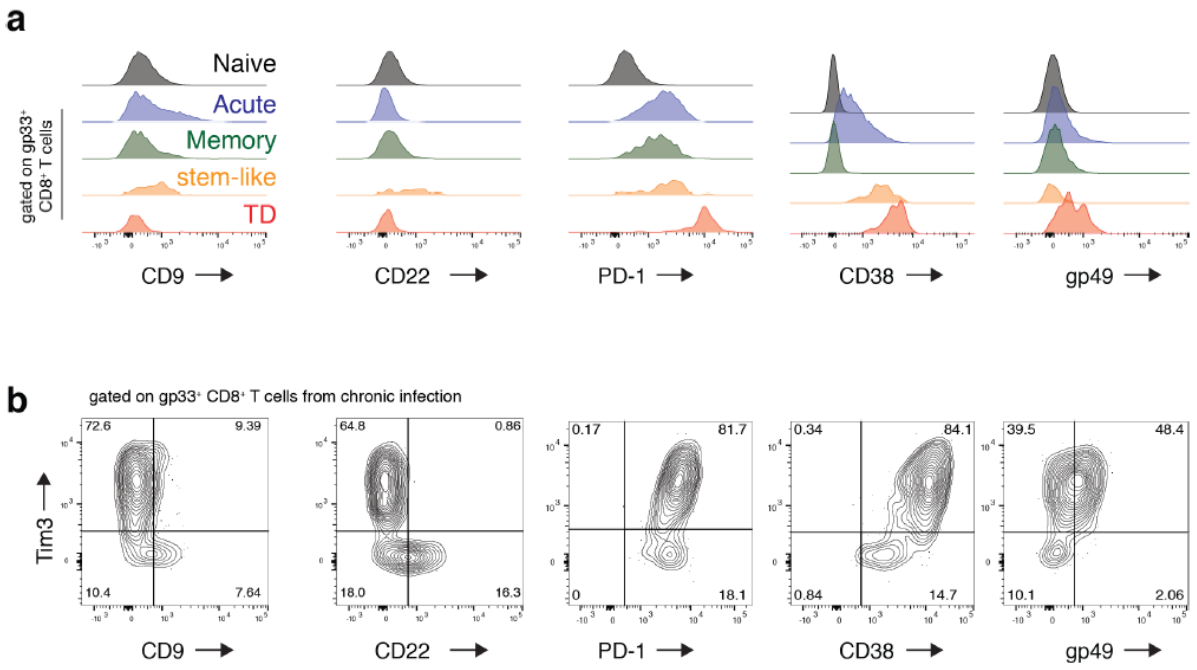

Figure 2: Flow cytometric confirmation of markers identified on LCMV-specific CD8⁺ T cells in chronic infection. Expression of CD9 and CD22, two markers identified on stem-like CD8⁺ T cells, and PD-1, gp49, and CD38, three markers identified on Tim3⁺ terminally differentiated CD8⁺ T cells is shown. a) Expression of each marker on CD8⁺ T cells. Naive cells are from uninfected mice; acute and memory samples are day 8 and >45 from LCMV Armstrong infection, and stem-like and terminally differentiated (TD) cells are from day >45 of LCMV clone 13 infection. b) Co-expression of each marker with Tim3 at day >45 after LCMV clone 13 infection, gated on LCMV-specific (gp33⁺) CD8⁺ T cells.

CD101 is specifically induced on CD8⁺ T cells in chronic viral infection

Of the markers whose protein expression was confirmed by flow cytometry, CD101 exhibited a unique expression pattern on LCMV-specific CD8⁺ T cells from chronic infection (**Figure 3a**). While stem-like CD8⁺ T cells did not express CD101, Tim3⁺ cells exhibited bimodal expression of CD101, with most Tim3⁺ cells expressing CD101 at later stages of chronic infection (day >45 post-infection, p.i.) (**Figure 3a**). To determine kinetics of CD101 induction, we infected C57BL/6JB6 (B6) mice with LCMV clone 13 or LCMV Armstrong and analyzed CD101 expression on splenic LCMV-specific CD8⁺ T cells (**Figure 3b**).

Eight days after infection, expression of CD101 was not detected on LCMV-specific cells in mice with acute or chronic infection. By day 15 post-infection, CD101 was detectable on a small subset of Tim3⁺ LCMV-specific CD8⁺ T cells in chronically infected mice. At 3 and 4 weeks after induction of chronic infection, most Tim3⁺ cells also expressed CD101. In stark contrast, CD101 was undetectable on LCMV-specific CD8⁺ T cells at any time point during acute infection (**Figure 3c**).

In other organs, CD101 was induced at similar time points in chronic infection, with detectable expression two weeks after infection and prominent CD101⁺Tim3⁺ populations 3-4 weeks after infection (**Figure 3d**). As in spleen, CD101 was not detected on LCMV-specific CD8⁺ T cells at any time point following acute infection in liver. Late in chronic infection (day >45 after infection), CD101⁺ LCMV-specific cell numbers differed among tissues, with lung containing the lowest frequency of CD101⁺Tim3⁺ cells, and bone marrow and liver the highest (**Figure 3e**). The frequencies of these populations among organs did not substantially differ between gp33-specific and gp276-specific CD8⁺ T cells (**Figure 3e**), and CD101⁺Tim3⁻ cells were rarely observed.

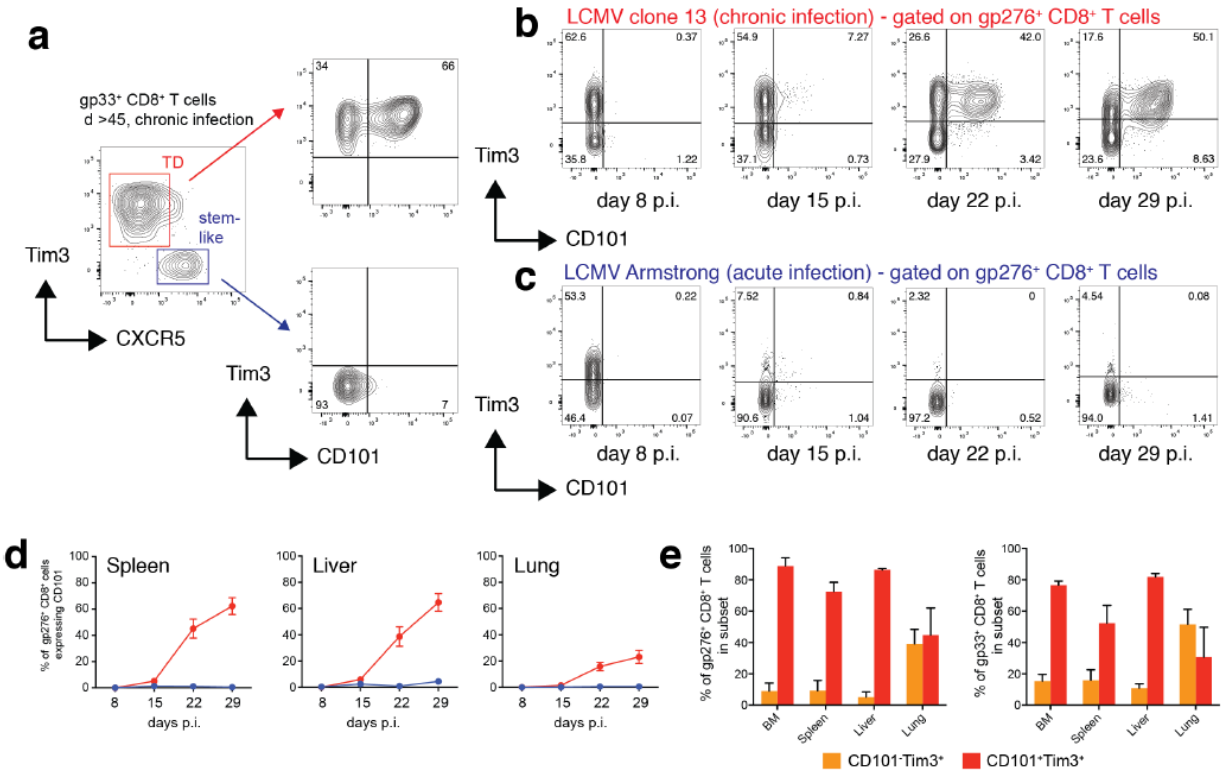

Figure 3: CD101 is induced on virus-specific CD8$^+$ T cells exclusively during chronic infection and defines two populations of Tim3$^+$ cells. a) Flow cytometry showing CD101 expression on the stem-like and Tim3$^+$ terminally differentiated (TD) subsets of LCMV-specific (gp33$^+$) CD8$^+$ T cells in chronic infection. b) Representative CD101 and Tim3 expression on endogenous D^{b}gp276-specific cells eight, 15, 22, and 29 days after infection with LCMV clone 13. c) CD101 and Tim3 expression on endogenous D^{b}gp276-specific cells eight, 15, 22, and 29 days after infection with LCMV Armstrong. d) Percentage of gp276$^+$ CD8$^+$ T cells from indicated organs expressing CD101 after infection with clone 13 (red) or Armstrong (blue). e) >45 days after infection with LCMV clone 13 and CD4 depletion, lymphocytes were isolated from multiple tissues. The percentage of CD101$^-$Tim3$^+$ and CD101$^+$Tim3 cells among gp33-specific CD8 T cells and gp276-specific CD8 T cells were determined by flow cytometry. Panels d and e show mean ± SEM.

CD101 expression defines transcriptionally distinct antigen-specific CD8$^+$ T cells

To identify transcriptional differences between stem-like (PD-1$^+$CD101$^-$Tim3$^+$), PD-1$^+$CD101$^-$Tim3$^+$, and PD-1$^+$CD101$^+$Tim3$^+$ CD8$^+$ T cells, we used FACS to isolate these three subsets of PD-1$^+$CD8$^+$ T cells from spleens of chronically infected mice and naive CD8$^+$ T cells from uninfected mice. 1,825 genes were differentially expressed between CD101$^-$Tim3$^+$ and CD101$^+$Tim3$^+$ PD-1$^+$CD8$^+$ T cells (**Figure 4a**), indicating that CD101 expression defines two transcriptionally distinct populations of Tim3$^+$ CD8$^+$ T cells in chronic infection. Notably, *Cd101* was the most differentially expressed gene between the two groups as measured both by adjusted p-value and fold change (**Figure 4a**).

To broadly compare the transcriptional profile of naive, stem-like, and CD101$^{-/+}$ Tim3$^+$ CD8$^+$ T cells, we performed principal component analysis (PCA) on these samples, which identified three principal components explaining 10% or more of transcriptional variance among samples (**Figure 4b**). CD101$^-$ and CD101$^+$ Tim3$^+$ cells were similarly situated on the first principal component (PC_1), which explains 46% of transcriptional variance among all cell types measured (**Figure 4c**). However, the two Tim3$^+$ subsets differed on PC_2 and PC_3, which collectively explain a third of transcriptional variance (**Figure 4c**). Specifically, CD101$^-$Tim3$^+$ cells were similar to naive cells on PC_2 and stem-like cells on PC_3, suggesting that CD101$^-$Tim3$^+$ cells may retain some transcriptional programs similar to these other cell types.

We also examined individual gene expression in each of the four sequenced subsets (**Figure 4d**). Expression of some genes, such as *Tcf7* (encoding Tcf-1) was shared by stem-like and naive cells, whereas others such as *Cxcr5* were expressed only in stem-like cells. Many effector genes such as *Prf1* (encoding perforin) were expressed in both CD101$^-$ and CD101$^+$ Tim3$^+$ cells,

with much lower expression in stem-like cells. Notably, several genes were expressed predominately or exclusively in CD101^{-}Tim3^{+} cells, such as *Cx3cr1* and *Tbx21*, which encodes T-bet (**Figure 4d**). Another striking pattern includes the very high expression of surface inhibitory molecules in CD101^{+} cells. Flow cytometric validation of selected differentially expressed proteins consistently confirmed RNA-sequencing results (**Figure 4e**). These results showed that stem-like, CD101^{-}Tim3^{+}, and CD101^{+}Tim3^{+} CD8^{+}T cells are three transcriptionally distinct populations of antigen-specific cells in chronic infection.

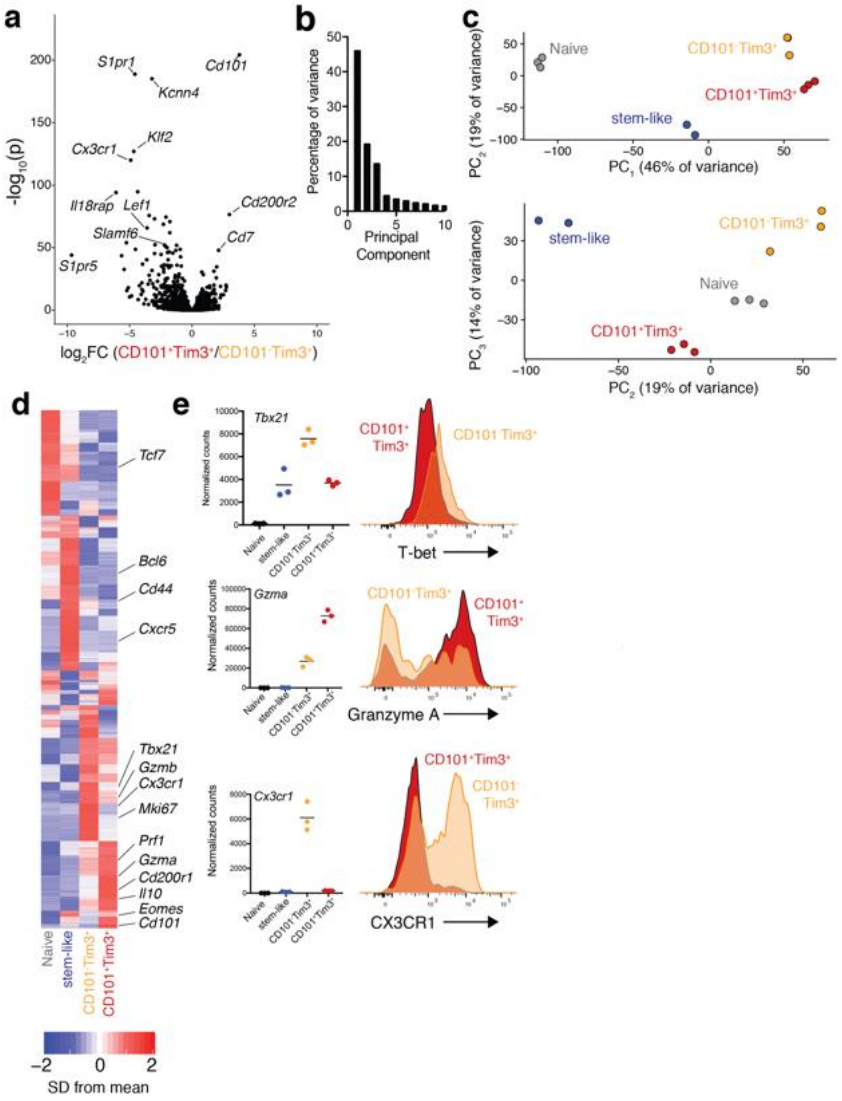

Figure 4: Distinctive transcriptional signatures define stem-like, CD101$^-$Tim3$^+$, and CD101$^+$Tim3$^+$ CD8$^+$ T cells.

RNA was isolated and sequenced from PD-1$^+$CD8$^+$ T cells of LCMV clone 13-infected mice (day >45). a) Volcano plot showing differential gene expression between CD101$^+$ Tim3$^+$ and CD101$^-$Tim3$^+$ cells; 1,825 genes were differentially expressed between these two subsets. b) Principal component analysis (PCA) identified three principal components that explained large amounts of transcriptional variance; samples are plotted on these components in panel (c). d) Heatmap shows mean relative expression of all differentially expressed genes across the four sequenced groups. e) Confirmation of selected differentially-expressed protein-coding genes by flow cytometry. Left, normalized counts (RNA-sequencing) of each gene. Right, flow cytometry staining of each marker, gated on gp33-specific CD8$^+$ T cells from spleens of chronically-infected mice.

CD101$^-$Tim3$^+$ cells are a transitory CD8$^+$ T cell population arising from Tcf-1$^+$ stem-like cells

Based on the transcriptional signatures of cell division and effector function present in CD101$^-$Tim3$^+$ cells and the highly exhausted signature of CD101$^+$ Tim3$^+$ cells, we hypothesized that CD101$^-$Tim3$^+$ cells are a transitory population in the differentiation pathway between stem-like Tim3$^-$ CD8$^+$ T cells and fully exhausted CD101$^+$Tim3$^+$ CD8$^+$ T cells. To test this hypothesis, we performed adoptive transfer of cells from the above subsets from chronically infected mice into congenically-distinct, infection-matched mice (**Figure 5a**). Splenocytes were isolated from CD45.2$^+$ B6 mice chronically infected with LCMV clone 13 and labeled with CellTrace Violet (CTV), a proliferation tracking dye. Using FACS, we separated three populations of PD-1$^+$CD8$^+$ T cells: CD101$^-$Tim3$^-$ stem-like cells, CD101$^-$Tim3$^+$ cells, and CD101$^+$Tim3$^+$ cells. These cells were then transferred intravenously into separate chronically-infected, congenically distinct CD45.1$^+$ recipient mice (**Figure 5a**). Two weeks post-transfer, lymphocytes were isolated from spleen, liver, lungs, and bone marrow of recipient mice and donor cells were analyzed by flow cytometry for expression of Tim3, CD101, and CTV dilution (**Figure 5b-c**).

Stem-like donor CD8$^+$ T cells maintained a CD101$^-$Tim3$^-$ phenotype or differentiated into CD101$^-$Tim3$^+$ or CD101$^+$Tim3$^+$ cells (**Figure 5b**). In spleen and bone marrow, most stem-like donor cells retained their pre-transfer phenotype, whereas most of those recovered in lung and liver expressed Tim3$^+$. Most donor stem-like cells recovered in lung and liver had also diluted CTV, often to the maximum detectable extent, which represents eight or more rounds of division (**Figure 5c**). In spleen and bone marrow, most recovered stem-like cells had not divided.

Recovered CD101$^-$Tim3$^+$ donor cells either kept their CD101$^-$Tim3$^+$ phenotype or converted into CD101$^+$Tim3$^+$ cells. In bone marrow and liver, the majority of donor CD101$^-$Tim3$^+$

recovered cells upregulated CD101, but only a very small fraction of cells found in the lung upregulated CD101 (**Figure 5b**). These results mirror the frequency of endogenous $CD101^{-}Tim3^{+}$ cells (**Figure 3e**), suggesting that tissue environment may play a major role on $CD8^{+}$ T cell differentiation in chronic viral infection. $CD101^{-}Tim3^{+}$ cells were also capable of division *in vivo*, as approximately half of these cells had diluted CTV, with some variation by tissue (**Figure 5c**). Some donor $CD101^{-}Tim3^{+}$ cells had diluted CTV to the maximum detectable extent, although this fraction was much smaller than those seen after transfer of stem-like cells.

Finally, transferred $CD101^{+}Tim3^{+}$ cells were exclusively recovered in the $CD101^{+}Tim3^{+}$ state, demonstrating that CD101 is an irreversible marker of exhausted cells (**Figure 5b**). Additionally, most of these donor cells had not diluted CTV (**Figure 5c**), nor were any of these cells capable of completely diluting CTV. Together, these results confirm previous experiments demonstrating the differentiation of $PD\text{-}1^{+}$ stem-like cells to $PD\text{-}1^{+}Tim3^{+}$ state (Im et al., 2016). These results also demonstrate that stem-like cells initially differentiate into transitory $CD101^{-}Tim3^{+}$ cells. These transitory cells then convert into fully exhausted $CD101^{+}Tim3^{+}$ cells with extremely limited potential for division and no ability to revert into $CD101^{-}Tim3^{+}$ cells.

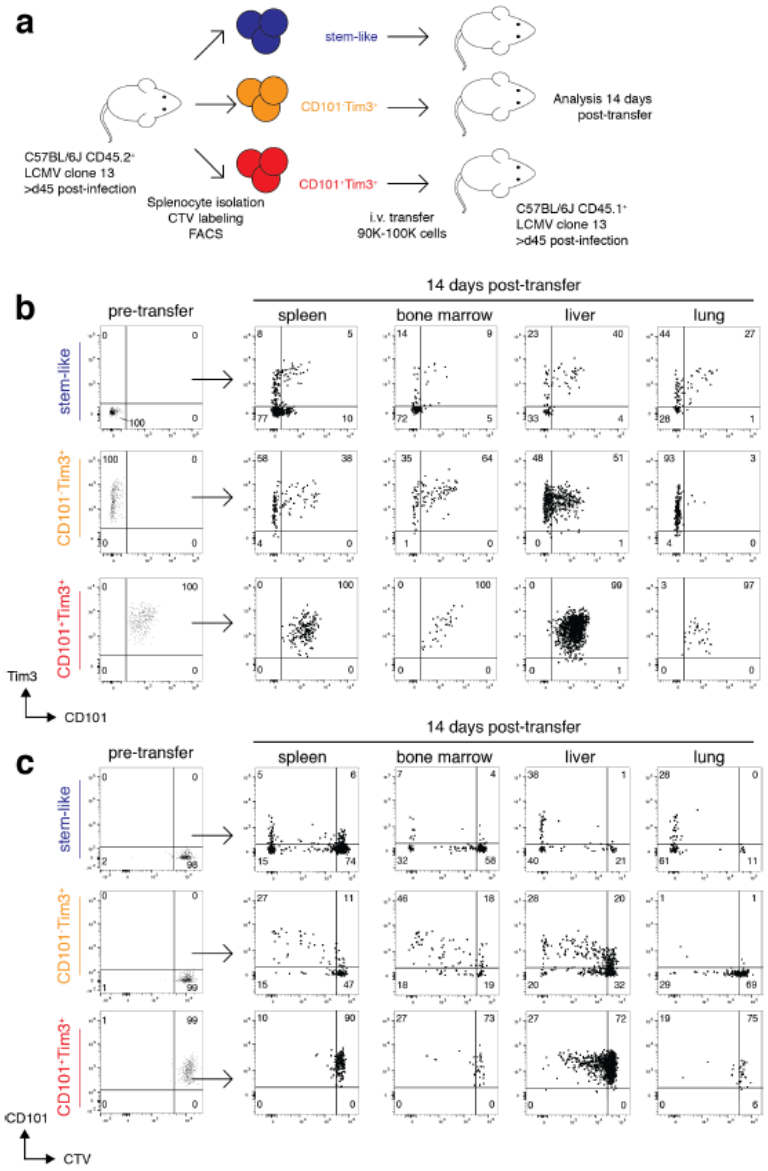

Figure 5: Stem-like CD8$^+$ T cells differentiate into transitory CD101$^-$Tim3$^+$ cells, followed by irreversible conversion into exhausted CD101$^+$Tim3$^+$ cells. a) PD-1$^+$ CD8$^+$ T cells were collected from spleens of mice chronically infected with LCMV clone 13 and labeled with CellTrace Violet (CTV). From these, three subsets (CD101$^-$Tim3$^-$, CD101$^-$Tim3$^+$, and CD101$^+$Tim3$^+$) were isolated via FACS and transferred intravenously to infection-matched, congenically distinct mice. Recipient mice were sacrificed two weeks after transfer to analyzed phenotype of donor cells. b-c) Phenotype (b) and CTV staining (c) of adoptively transferred cells at transfer. All populations shown are gated on PD-1$^+$CD45.2$^+$CD45.1$^-$ CD8$^+$ T cells. Cells shown are pooled from all recipient mice from one independent experiment, and results are representative of two independent experiments.

Newly-generated CD101^{-}Tim3^{+} CD8^{+} T cells are more functional CD101^{+}Tim3^{+} CD8^{+} T cells

Given the findings from the adoptive transfer experiment, our gene expression analysis above provides insight into the transcriptional changes occurring during CD8^{+} T cell differentiation in chronic viral infection (**Figure 6a**). Upon division and differentiation of stem-like cells to transitory CD101^{-}Tim3^{+} cells, the expression of migration-associated (*Cx3cr1*, *Ccr2, Itgam*, *Itga6*) and division-associated (*Mki67, Mcm2-7*, *Aurkb*) genes is upregulated. Expression of some exhaustion markers such as PD-1, CD112R, and TIGIT are also upregulated, coinciding with downregulation of CD28, a co-stimulatory molecule. Upon differentiation of transitory CD101^{-} Tim3^{+} cells to exhausted CD101^{+}Tim3^{+} cells, migration- and division-associated genes are downregulated. The levels of key transcription factors also change during this course differentiation, with stem-like cells characterized by expression of Tcf-1 and transitory cells characterized by high levels migration-associated genes, T-bet and Klf2. Exhausted CD101^{+}Tim3^{+} downregulate Klf2 and T-bet and highly express Runx3, Stat3, Irf1, and Hic1. Finally, inhibitory molecules PD-1, CD112R, and TIGIT are further upregulated in exhausted CD101^{+}Tim3^{+} cells compared to transitory cells, and other inhibitory molecules such as CD160, Lag3, and CD200R1 are only upregulated in highly exhausted cells compared to stem-like cells (**Figure 6a)**.

Flow cytometry analysis confirmed this higher expression of many inhibitory molecules, including 2B4 (CD244), CD160, and CD200R(1) (**Figure 6b**). Ki-67 staining was most prominent in transitory cells, as predicted by RNA-sequencing analysis (**Figure 6a,c**). This finding was similar in LCMV-specific CD8^{+} T cells isolated from spleen, liver and lung during chronic infection (**Figure 6c-d**). This is consistent with a differentiation pathway in which resting stem-like CD8^{+} T cells infrequently divide and convert into rapidly proliferating transitory CD101^{-}Tim3^{+} cells. These cells

then lose proliferative potential upon conversion to $CD101^{+}Tim3^{+}$ cells, as evidenced by their lower steady-state Ki-67 expression (**Figure 6c-d**). Interestingly, we found that Ki-67^{+} $CD101^{+}$ $CD8^{+}$ T cells expressed lower levels of CD101 than Ki-67^{-} $CD101^{+}$ cells, suggesting that onset of dysfunction is paired with gradual upregulation of CD101 (**Figure 7**).

To determine the ability of the different $CD8^{+}$ T cell subsets to produce effector cytokines during chronic infection, we stimulated splenocytes from mice infected with LCMV clone 13 with their cognate peptide antigen, gp33 (**Figure 6e**). Twenty-two days post-infection, approximately 70% and 60% of stem-like and transitory P14 cells, respectively, produced IFNγ. In contrast, only 20% of $CD101^{+}$ exhausted P14 cells were $IFN\gamma^{+}$ (**Figure 6f**). Of the cells producing IFNγ, $CD101^{+}$ $IFN\gamma^{+}$ cells produced significantly lower amounts of IFNγ compared to $IFN\gamma^{+}$ transitory or stem-like cells (**Figure 6g**). These experiments demonstrate that during chronic viral infection, stem-like cells differentiate into transitory $CD101^{-}Tim3^{+}$ cells that retain proliferative and effector capacity before irreversible conversion into fully exhausted $CD101^{+}$ cells with extremely limited capacity for division and cytokine production.

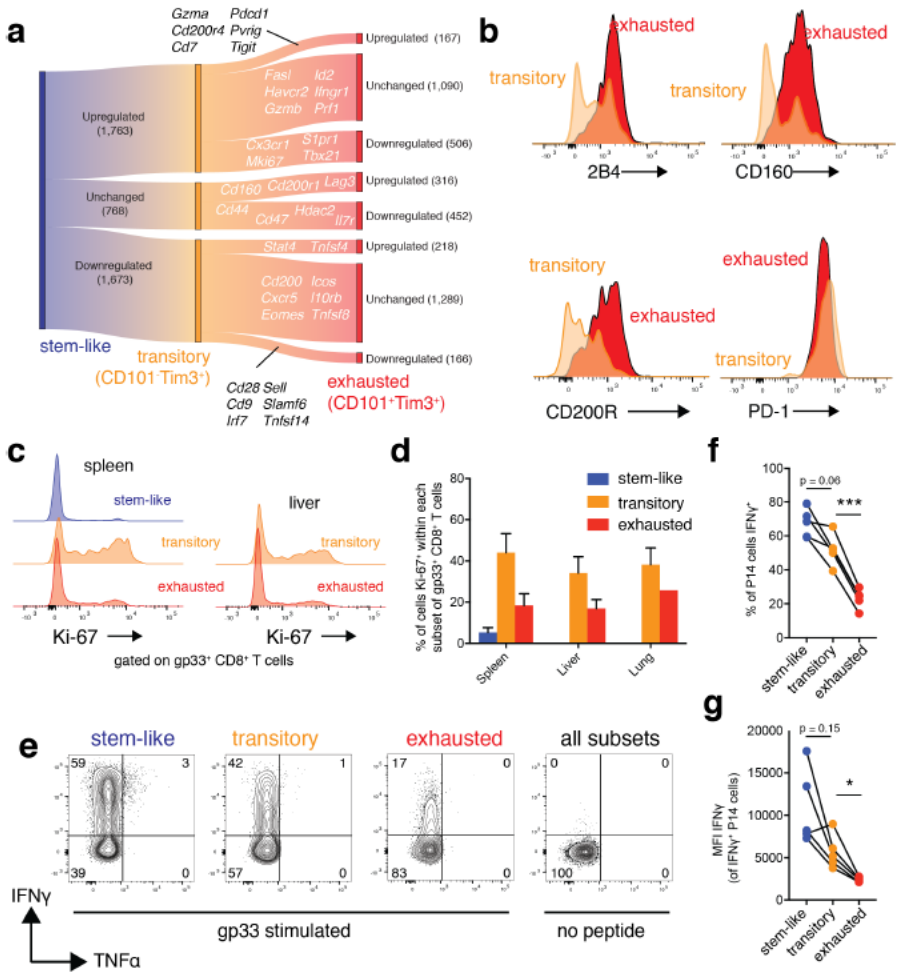

Figure 6: Transitory CD8⁺ T cells in chronic infection retain proliferative capacity and are more functional than CD101⁺Tim3⁺ cells. a) Plot showing changes in gene expression during CD8⁺ T cell differentiation from stem-like cells to transitory CD101⁻Tim3⁺ cells and subsequent conversion to exhausted CD101⁺Tim3⁺ cells. Selected differentially expressed genes are shown. b) Expression of selected surface exhaustion markers in transitory (orange) and exhausted CD101⁺Tim3⁺ cells (red). Populations are gated on gp33⁺ CD8⁺ T cells from chronic infection. c) Ki-67 expression in subsets of gp33-specific CD8⁺ T cells isolated from spleen and liver. d) Summary data of Ki-67 staining of gp33⁺ CD8⁺ T cells from chronic infection. e) P14 cells were transferred to B6 mice. Twenty-two days after infection, splenocytes were isolated and stimulated with gp33 peptide or a no-peptide control, and subsets analyzed by flow cytometry for cytokine expression. f) Percentage of P14 cells expressing IFNγ by subset. g) MFI of IFNγ staining on IFNγ⁺ cells within each subset. Statistics shown are one-way ANOVA with Tukey's test for multiple comparisons. * indicates $p < 0.05$ and *** indicates $p < 0.001$. Panel (d) shows mean ± SEM.

Numbers of virus-specific transitory cells increase after PD-1 pathway blockade

In chronic LCMV infection, PD-1 pathway blockade leads to improved viral control and increased proliferation and cytokine production by antigen-specific $CD8^+$ T cells (Barber et al., 2005). To observe the effects of PD-1 pathway blockade on our three exhausted subsets, we treated chronically infected B6 mice with αPD-L1 and analyzed antigen-specific $CD8^+$ T cells by flow cytometry. PD-1 pathway blockade resulted in an increase in total numbers of LCMV-specific $CD8^+$ T cells (**Figure 7a**). Previous work has shown that division of stem-like cells is responsible for the increase in antigen-specific $CD8^+$ T cells after blockade (Im et al., 2016).

After PD-1 blockade, we found both a higher frequency of antigen-specific $CD101^-Tim3^+$ cells (**Figure 7b**) as well as higher absolute numbers of these cells in spleen, liver, and lung compared to PBS-treated controls compared to the other two subsets (**Figure 7c**). As previously observed, we did not find a significant increase in stem-like cells in αPD-L1-treated mice compared to controls (Im et al., 2016) (**Figure 8a**). Numbers of $CD101^+Tim3^+$ exhausted cells increased after PD-1 pathway blockade, although $CD101^+Tim3^+$ cells were a smaller fraction of $Tim3^+$ cells in treated mice compared to controls (**Figure 7b**). Thus, PD-1 pathway blockade leads to increased numbers of effector-like cells, including the transitory subset which is capable of proliferation and effector cytokine production.

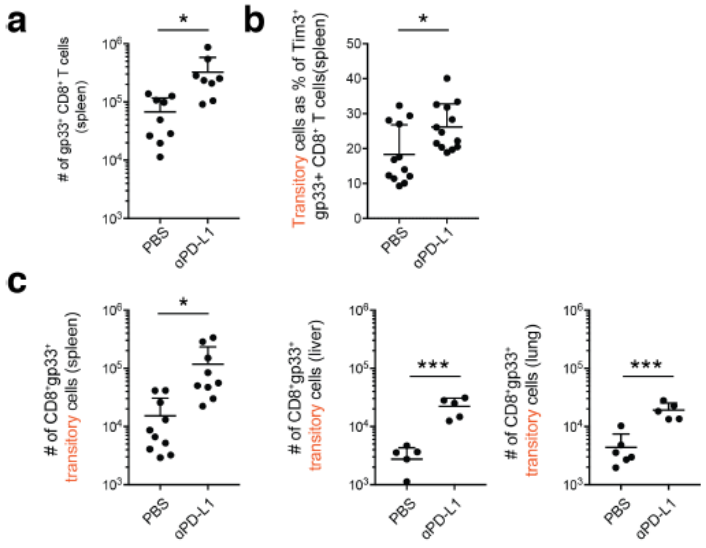

Figure 7: PD-1 pathway blockade increases the number of transitory antigen-specific CD8⁺ T cells.

Chronically infected mice were treated with αPD-L1 or PBS. a) Total numbers of gp33⁺ CD8⁺ T cells from spleen. b) Frequency of transitory CD101⁻Tim3⁺ cells among total Tim3⁺ gp33⁺ CD8⁺ T cells in spleen. c) Numbers of gp33-specific transitory CD101⁻Tim3⁺ cells in spleen, liver, and lung.

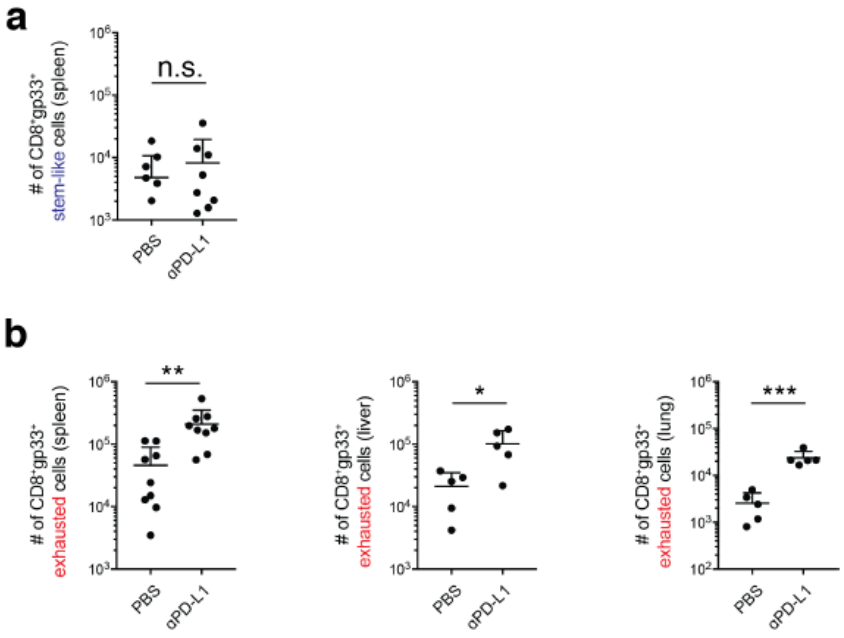

Figure 8: PD-1 pathway blockade increases the number of CD101⁺Tim3⁺ antigen-specific CD8⁺ T cells but not stem-like cells. Chronically infected mice were treated with αPD-L1 or PBS. a) Numbers of gp33-specific stem-like CD8⁺ T cells in spleen. b) Numbers of gp33-specific exhausted CD101⁺Tim3⁺ cells in spleen, liver, and lung.

Discussion

We performed a systematic analysis to define surface molecules that are preferentially expressed on exhausted $CD8^+$ T cells. This analysis confirmed known checkpoint molecules, such as PD-1 and Lag3, but also identified a host of other molecules whose function in $CD8^+$ T cell exhaustion is less well studied. However, many of these molecules, such as Lax1, CD7, CD200R, CD112R, and CD101 have been shown to inhibit TCR signaling or otherwise impair T cell function (Pace et al., 2000; Rosenblum et al., 2005; Rygiel et al., 2009; Soares et al., 1998; Zhu et al., 2002; Zhu et al., 2016). A recent study using a liver tumor mouse model identified CD101 as a marker of antigen-specific $CD8^+$ T cells with a dysfunctional chromatin state (Philip et al., 2017). It is unclear whether CD101 is merely a marker of dysfunctional cells or contributes to negative regulatory signaling itself, although evidence points to its role as inhibitory molecule on T cells *in vitro* and *in vivo* (Mohammed et al., 2011; Rainbow et al., 2011; Schey et al., 2016; Soares et al., 1998). Here, we demonstrate that CD101 defines terminally differentiated, exhausted $CD8^+$ T cells in chronic viral infection.

Initially, stem-like Tcf-1^+ $CD8^+$ T cells present in chronic viral infection differentiate into transitory $CD101^-Tim3^+$ cells, a process accelerated by PD-1 pathway blockade (Im et al., 2016). RNA-sequencing analyses show that upon differentiation from stem-like cells, transitory cells downregulate Tcf-1 and express transcriptional programs for cytotoxicity, cell proliferation, and migration as shown by GSEA and expression of genes encoding Ki-67, Gzmb, S1pr1, and CX3CR1 (**Figure 4g**). These cells also contain high levels of effector- and migration-associated transcription factors, such as T-bet (Sullivan et al., 2003) and Klf2 (Carlson et al., 2006). Interestingly, a recent report identified increased numbers of circulating $Gzmb^{hi}$ $CX3CR1^+$ $CD8^+$ T cells in cancer patients

who responded to PD-1 blockade therapy (Yan et al., 2018). We also show that transitory cells increase in numbers after PD-1 blockade and are capable of division and cytokine production in chronically infected mice, although it is unclear how similar these transitory cells in mice are to human CX3CR1$^+$ CD8$^+$ T cells after PD-1 blockade.

With continued persistence of antigen during chronic infection, transitory antigen-specific CD8$^+$ T cells convert into particularly dysfunctional CD101$^+$ cells (**Figure 5**). This transition involves downregulation of migratory molecules such as S1pr1 and Cx3cr1 and expression of an alternate, exhaustion-associated program. Klf2 and T-bet are downregulated while Runx3 and Hic1 are upregulated which may program non-lymphoid residency and transcriptional repression of effector molecules, respectively (Milner et al., 2017; Ubaid et al., 2018). In addition, expression of well-known surface markers of exhaustion such as CD160, 2B4, and PD-1 as well as the novel dysfunction-associated markers described here (CD200Rs, CD7, Lax1, CD112R, etc.) is universally increased in exhausted CD101$^+$Tim3$^+$ cells.

This finding suggests that in addition to proteins associated with exhaustion such as PD-1 and Tim3, other exhaustion-associated genes, including CD101, are upregulated on antigen-specific CD8$^+$ T cells weeks after initial antigen exposure. PD-1 expression is seen on antigen-specific T cells following acute infection (**Figure 2**) and can be observed on memory CD8$^+$ T cells hours after antigen exposure (Hosking et al., 2013). In contrast, CD101 is not induced until 2-4 weeks after induction of chronic viral infection and is not observed on LCMV-specific cells in acute infection (**Figure 3**). Thus, CD101 and its associated surface markers such as CD7 and the CD200 receptors may constitute a 'second wave' of inhibitory molecules induced on antigen-specific CD8$^+$ T cells weeks after infection. This observation also demonstrates that T cell exhaustion is a

gradual process with emergence of highly dysfunctional $CD8^+$ T cells overtime. Steady-state levels of $CD101^+$ $CD8^+$ T cells do not appear until 3-4 weeks after infection (**Figure 3**); thus, immunological models that begin checkpoint blockade less than a month after viral or tumor inoculation may not show the full extent of $CD8^+$ T cell exhaustion present in chronic viral infection or the presence of additional putative inhibitory molecules present in the CD101-associated transcriptional program.

Finally, we show that PD-1 pathway blockade causes a dramatic increase of antigen-specific transitory $CD8^+$ T cells. This is consistent with recent findings that stem-like cells are responsible for the proliferative burst in response to PD-1 blockade (Im et al., 2016), as we show that these stem-like cells give rise to transitory effector cells with effector and proliferative capacity. Thus, both quality and quantity of $CD8^+$ T cells after checkpoint blockade therapy may be crucial for an effective response to immunotherapy *in vivo*.

Future Directions

While CD101 is a marker of this highly exhausted subset, its functional contribution to this dysfunctional cell phenotype is unknown. To better understand whether CD101 itself is causing this exhausted state, we generated T cell specific CD101 knockout (KO) mice and are currently monitoring their response to LCMV clone 13 infection. We propose that signaling through CD101 promotes this highly exhausted phenotype, marked by reduced proliferation, cytokine production, and cytotoxic capacity.

To determine the role of CD101 on $CD8^+$ T cell function, we will compare the phenotypes of CD101 KO and control $CD8^+$ T cells over the course of LCMV clone 13 infection (**Figure 9**). We will inject two types of cells, experimental $CD101^-$ cells and control $CD101^+$ cells from B6 mice, into wildtype (WT) B6 mice. Cells from each mouse will contain the P14 transgene, a transgenic T cell receptor specific for the LCMV epitope gp33. This allows for a well-controlled experiment as every donor T cell will respond to the LCMV infection within the context of infection of the same mouse.

After transfer, we will infect these mice with LCMV clone 13 intravenously, which causes a chronic infection. We will regularly monitor the mice and collect tissue samples at eight, 15 and 28 days post-infection, sacrificing the mice at day 45. We will process the tissues (spleen, liver, lung, bone marrow) and stain with fluorescent antibodies to visualize cellular phenotypes via flow cytometry.

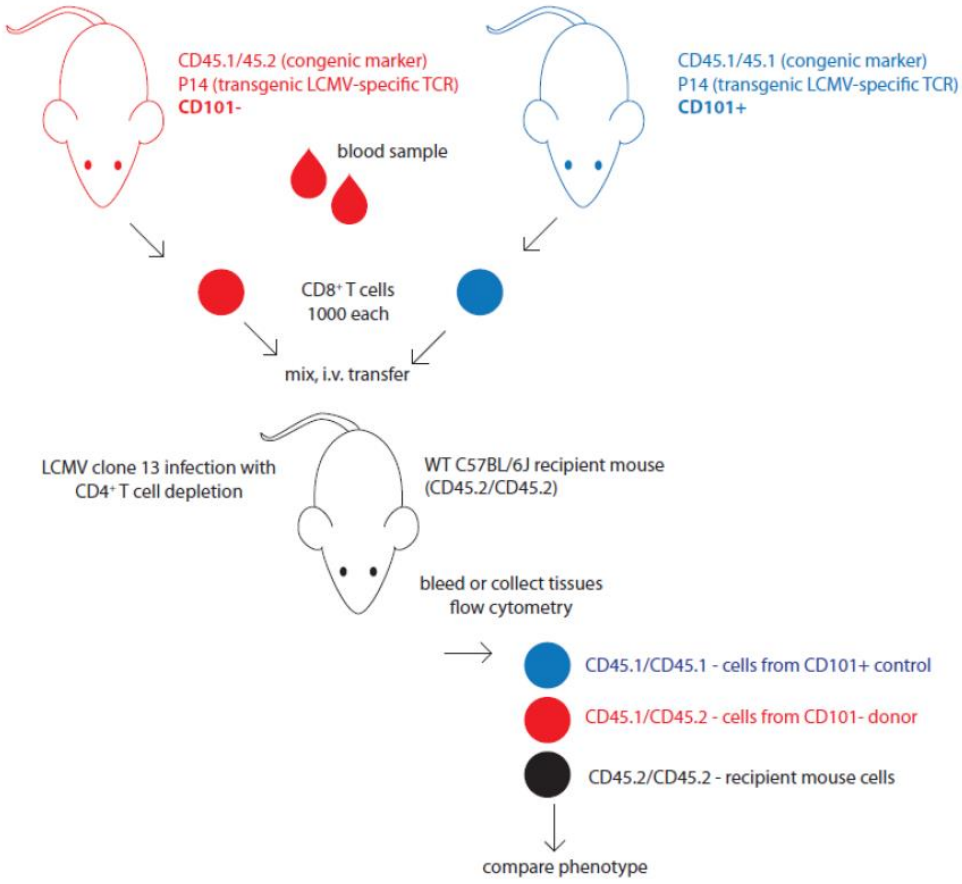

Figure 9. Proposed adoptive transfer of CD101 KO and control cells into WT recipient mouse.

Conclusion

After systematic analysis of surface molecules on exhausted $CD8^+$ T cells, we identified CD101 as a marker of particularly dysfunctional, terminally differentiated $CD8^+$ T cells. These $CD101^+Tim3^+$ cells arise from transitory $CD101^-Tim3^+$ cells during chronic viral infection and those, in turn, differentiate from a stem-like population of $CXCR5^+$ $PD1^+$ cells (**Figure 10**). CD101 expression correlates with an upregulation of well-known exhaustion markers including PD-1, CD160, and 2B4 and lower production of cytokines like IFNγ. Further, we show that CD101 expression is gradual, with steady-state levels of $CD101^+$ $CD8^+$ T cells not evident until 3-4 weeks post-infection; thus, immunological models that begin checkpoint blockade less than a month after viral or tumor inoculation may inadequately recapitulate the full extent of $CD8^+$ T cell exhaustion present in chronic viral infection.

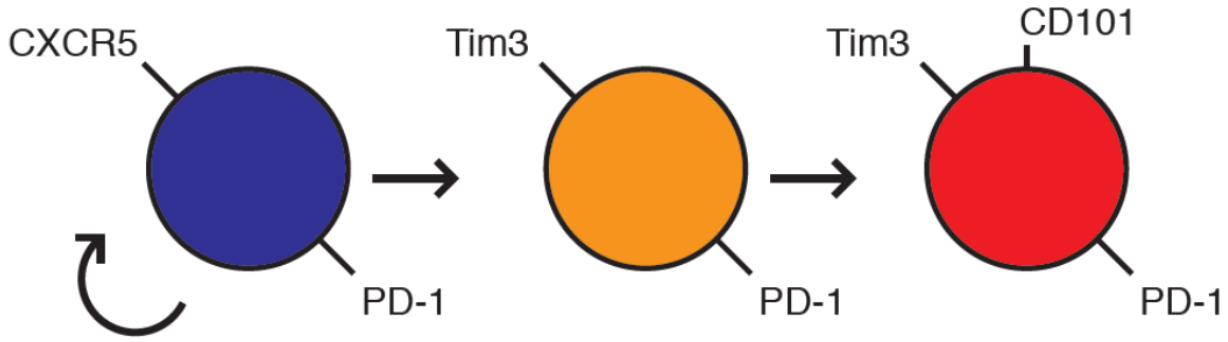

Figure 10. Stem-like cells differentiate into $CD101^-Tim3^+$ cells before final and irreversible progression into $CD101^+Tim3^+$ cells.

While these studies identify CD101 as a marker of dysfunctional cells, the exact role of CD101 related to these dysfunctional cellular phenotypes is unknown. Thus, we will generate CD101 KO mice and compare their response to chronic viral infection and their cellular phenotype using an adoptive transfer mouse model. We will measure cytokine production,

proliferation, and gene expression of cells with and without CD101 to determine if CD101 has a causative role in promoting this highly exhausted phenotype. If our hypothesis is correct, CD101 blockade has the potential to be a beneficial immunotherapy for tumors resistant to PD-1 blockade.

References

Akondy, R.S., Fitch, M., Edupuganti, S., Yang, S., Kissick, H.T., Li, K.W., Youngblood, B.A., Abdelsamed, H.A., McGuire, D.J., Cohen, K.W., et al. (2017). Origin and differentiation of human memory CD8 T cells after vaccination. *Nature* 552, 362-367.

Araki, K., Morita, M., Bederman, A.G., Konieczny, B.T., Kissick, H.T., Sonenberg, N., and Ahmed, R. (2017). Translation is actively regulated during the differentiation of CD8+ effector T cells. *Nature Immunology*.

Barber, D.L., Wherry, E.J., Masopust, D., Zhu, B., Allison, J.P., Sharpe, A.H., Freeman, G.J., and Ahmed, R. (2005). Restoring function in exhausted CD8 T cells during chronic viral infection. *Nature* 439, 682-687.

Barclay, A.N. (2003). Membrane proteins with immunoglobulin-like domains—a master superfamily of interaction molecules. *Seminars in Immunology* 15, 215-223.

Brahmer, J.R., Tykodi, S.S., Chow, L.Q.M., Hwu, W.-J., Topalian, S.L., Hwu, P., Drake, C.G., Camacho, L.H., Kauh, J., Odunsi, K., et al. (2012). Safety and Activity of Anti–PD-L1 Antibody in Patients with Advanced Cancer. *New England Journal of Medicine* 366, 2455-2465.

Brummelman, J., Mazza, E.M.C., Alvisi, G., Colombo, F.S., Grilli, A., Mikulak, J., Mavilio, D., Alloisio, M., Ferrari, F., Lopci, E., et al. (2018). High-dimensional single cell analysis identifies stem-like cytotoxic CD8+ T cells infiltrating human tumors. *The Journal of Experimental Medicine* 215, 2520-2535.

Callahan, M.K., and Wolchok, J.D. (2013). At the Bedside: CTLA-4- and PD-1-blocking antibodies in cancer immunotherapy. *Journal of Leukocyte Biology* 94, 41-53.

Carlson, C.M., Endrizzi, B.T., Wu, J., Ding, X., Weinreich, M.A., Walsh, E.R., Wani, M.A., Lingrel, J.B., Hogquist, K.A., and Jameson, S.C. (2006). Kruppel-like factor 2 regulates thymocyte and T-cell migration. *Nature* 442, 299-302.

Chatterjee, M., Kis-Toth, K., Thai, T.-H., Terhorst, C., and Tsokos, G.C. (2011). SLAMF6-driven co-stimulation of human peripheral T cells is defective in SLE T cells. *Autoimmunity* 44, 211-218.

Day, C.L., Kaufmann, D.E., Kiepiela, P., Brown, J.A., Moodley, E.S., Reddy, S., Mackey, E.W., Miller, J.D., Leslie, A.J., DePierres, C., et al. (2006). PD-1 expression on HIV-specific T cells is associated with T-cell exhaustion and disease progression. *Nature* 443, 350-354.

Durinck, S., Moreau, Y., Kasprzyk, A., Davis, S., De Moor, B., Brazma, A., and Huber, W. (2005). BioMart and Bioconductor: a powerful link between biological databases and microarray data analysis. *Bioinformatics* 21, 3439-3440.

Durinck, S., Spellman, P.T., Birney, E., and Huber, W. (2009). Mapping identifiers for the integration of genomic datasets with the R/Bioconductor package biomaRt. *Nat Protoc* 4, 1184-1191.

Finn, R.D., Coggill, P., Eberhardt, R.Y., Eddy, S.R., Mistry, J., Mitchell, A.L., Potter, S.C., Punta, M., Qureshi, M., Sangrador-Vegas, A., et al. (2016). The Pfam protein families database: towards a more sustainable future. *Nucleic Acids Research* 44, D279-D285.

Gettinger, S.N., Choi, J., Mani, N., Sanmamed, M.F., Datar, I., Sowell, R., Du, V.Y., Kaftan, E., Goldberg, S., Dong, W., et al. (2018). A dormant TIL phenotype defines non-small cell lung carcinomas sensitive to immune checkpoint blockers. *Nature Communications* 9.

He, R., Hou, S., Liu, C., Zhang, A., Bai, Q., Han, M., Yang, Y., Wei, G., Shen, T., Yang, X., et al. (2016). Follicular CXCR5-expressing CD8+ T cells curtail chronic viral infection. *Nature* 537, 412-416.

Hosking, M.P., Flynn, C.T., Botten, J., and Whitton, J.L. (2013). CD8+ Memory T Cells Appear Exhausted within Hours of Acute Virus Infection. *The Journal of Immunology* 191, 4211-4222.

Hudson, W.H., Prokhnevska, N., Gensheimer, J., Akondy, R., McGuire, D.J., Ahmed, R., and Kissick, H.T. (2019). Expression of novel long noncoding RNAs defines virus-specific effector and memory CD8+ T cells. *Nature Communications* 10, 196.

Im, S.J., Hashimoto, M., Gerner, M.Y., Lee, J., Kissick, H.T., Burger, M.C., Shan, Q., Hale, J.S., Lee, J., Nasti, T.H., et al. (2016). Defining CD8+ T cells that provide the proliferative burst after PD-1 therapy. *Nature* 537, 417-421.

Jiang, H., Li, L., Han, J., Sun, Z., Rong, Y., and Jin, Y. (2017). CXCR5+ CD8+ T Cells Indirectly Offer B Cell Help and Are Inversely Correlated with Viral Load in Chronic Hepatitis B Infection. DNA and *Cell Biology* 36, 321-327.

Joshi, N.S., Cui, W., Chandele, A., Lee, H.K., Urso, D.R., Hagman, J., Gapin, L., and Kaech, S.M. (2007). Inflammation Directs Memory Precursor and Short-Lived Effector CD8+ T Cell Fates via the Graded Expression of T-bet Transcription Factor. *Immunity* 27, 281-295.

Kaech, S.M., Tan, J.T., Wherry, E.J., Konieczny, B.T., Surh, C.D., and Ahmed, R. (2003). Selective expression of the interleukin 7 receptor identifies effector CD8 T cells that give rise to long-lived memory cells. *Nature Immunology* 4, 1191-1198.

Kaech, S.M., Wherry, E.J., and Ahmed, R. (2002). Effector and memory T-cell differentiation: implications for vaccine development. *Nature Reviews Immunology* 2, 251-262.

Kim, D., Langmead, B., and Salzberg, S.L. (2015). HISAT: a fast spliced aligner with low memory requirements. *Nature Methods* 12, 357-360.

Krogh, A., Larsson, B., von Heijne, G., and Sonnhammer, E.L. (2001). Predicting transmembrane protein topology with a hidden Markov model: application to complete genomes. *J Mol Biol* 305, 567-580.

Lê, S., Josse, J., and Husson, F. (2008). FactoMineR: An R Package for Multivariate Analysis. *Journal of Statistical Software* 25.

Leong, Y.A., Chen, Y., Ong, H.S., Wu, D., Man, K., Deleage, C., Minnich, M., Meckiff, B.J., Wei, Y., Hou, Z., et al. (2016). CXCR5+ follicular cytotoxic T cells control viral infection in B cell follicles. *Nature Immunology* 17, 1187-1196.

Liao, Y., Smyth, G.K., and Shi, W. (2013). featureCounts: an efficient general purpose program for assigning sequence reads to genomic features. *Bioinformatics* 30, 923-930.

Liberzon, A., Birger, C., Thorvaldsdóttir, H., Ghandi, M., Mesirov, Jill P., and Tamayo, P. (2015). The Molecular Signatures Database Hallmark Gene Set Collection. *Cell Systems* 1, 417-425.

Liberzon, A., Subramanian, A., Pinchback, R., Thorvaldsdottir, H., Tamayo, P., and Mesirov, J.P. (2011). Molecular signatures database (MSigDB) 3.0. *Bioinformatics* 27, 1739-1740.

Love, M.I., Huber, W., and Anders, S. (2014). Moderated estimation of fold change and dispersion for RNA-seq data with DESeq2. *Genome Biology* 15.

Milner, J.J., Toma, C., Yu, B., Zhang, K., Omilusik, K., Phan, A.T., Wang, D., Getzler, A.J., Nguyen, T., Crotty, S., et al. (2017). Runx3 programs CD8+ T cell residency in non-lymphoid tissues and tumours. *Nature*.

Mohammed, J.P., Fusakio, M.E., Rainbow, D.B., Moule, C., Fraser, H.I., Clark, J., Todd, J.A., Peterson, L.B., Savage, P.B., Wills-Karp, M., et al. (2011). Identification of Cd101 as a Susceptibility Gene for Novosphingobium aromaticivorans-Induced Liver Autoimmunity. *The Journal of Immunology* 187, 337-349.

Moskophidis, D., Lechner, F., Pircher, H., and Zinkernagel, R.M. (1993). Virus persistence in acutely infected immunocompetent mice by exhaustion of antiviral cytotoxic effector T cells. *Nature* 362, 758-761.

Murali-Krishna, K., Altman, J.D., Suresh, M., Sourdive, D.J.D., Zajac, A.J., Miller, J.D., Slansky, J., and Ahmed, R. (1998). Counting Antigen-Specific CD8 T Cells: A Reevaluation of Bystander Activation during Viral Infection. *Immunity* 8, 177-187.

Nguyen, J.T., Evans, D.P., Galvan, M., Pace, K.E., Leitenberg, D., Bui, T.N., and Baum, L.G. (2001). CD45 Modulates Galectin-1-Induced T Cell Death: Regulation by Expression of Core 2 O-Glycans. *The Journal of Immunology* 167, 5697-5707.

Ott, P.A., Hodi, F.S., Kaufman, H.L., Wigginton, J.M., and Wolchok, J.D. (2017). Combination immunotherapy: a road map. *Journal for ImmunoTherapy of Cancer* 5.

Pace, K.E., Hahn, H.P., Pang, M., Nguyen, J.T., and Baum, L.G. (2000). Cutting Edge: CD7 Delivers a Pro-Apoptotic Signal During Galectin-1-Induced T Cell Death. *The Journal of Immunology* 165, 2331-2334.

Pardoll, D.M. (2012). The blockade of immune checkpoints in cancer immunotherapy. *Nature Reviews Cancer* 12, 252-264.

Pardoll, D. (2011). Timeline: a decade of advances in immunotherapy. *Nature Medicine*, 17 (3): 296, 2.

Philip, M., Fairchild, L., Sun, L., Horste, E.L., Camara, S., Shakiba, M., Scott, A.C., Viale, A., Lauer, P., Merghoub, T., et al. (2017). Chromatin states define tumour-specific T cell dysfunction and reprogramming. *Nature* 545, 452-456.

Rainbow, D.B., Moule, C., Fraser, H.I., Clark, J., Howlett, S.K., Burren, O., Christensen, M., Moody, V., Steward, C.A., Mohammed, J.P., et al. (2011). Evidence that Cd101 Is an Autoimmune Diabetes Gene in Nonobese Diabetic Mice. *The Journal of Immunology* 187, 325-336.

Rosenblum, M.D., Woodliff, J.E., Madsen, N.A., McOlash, L.J., Keller, M.R., and Truitt, R.L. (2005). Characterization of CD200-Receptor Expression in the Murine Epidermis. *Journal of Investigative Dermatology* 125, 1130-1138.

Rygiel, T.P., Rijkers, E.S.K., de Ruiter, T., Stolte, E.H., van der Valk, M., Rimmelzwaan, G.F., Boon, L., van Loon, A.M., Coenjaerts, F.E., Hoek, R.M., et al. (2009). Lack of CD200 Enhances Pathological T Cell Responses during Influenza Infection. *The Journal of Immunology* 183, 1990-1996.

Sallusto, F., Lenig, D., Förster, R., Lipp, M., and Lanzavecchia, A. (1999). Two subsets of memory T lymphocytes with distinct homing potentials and effector functions. *Nature* 401, 708-712.

Sarkar, S., Kalia, V., Haining, W.N., Konieczny, B.T., Subramaniam, S., and Ahmed, R. (2008). Functional and genomic profiling of effector CD8 T cell subsets with distinct memory fates. *The Journal of Experimental Medicine* 205, 625-640.

Schey, R., Dornhoff, H., Baier, J.L.C., Purtak, M., Opoka, R., Koller, A.K., Atreya, R., Rau, T.T., Daniel, C., Amann, K., et al. (2016). CD101 inhibits the expansion of colitogenic T cells. *Mucosal Immunology* 9, 1205-1217.

Soares, L.R., Tsavaler, L., Rivas, A., and Engleman, E.G. (1998). V7 (CD101) ligation inhibits TCR/CD3-induced IL-2 production by blocking Ca2+ flux and nuclear factor of activated T cell nuclear translocation. *J Immunol* 161, 209-217.

Subramanian, A., Tamayo, P., Mootha, V.K., Mukherjee, S., Ebert, B.L., Gillette, M.A., Paulovich, A., Pomeroy, S.L., Golub, T.R., Lander, E.S., and Mesirov, J.P. (2005). Gene set enrichment analysis: a knowledge-based approach for interpreting genome-wide expression profiles. *Proc Natl Acad Sci U S A* 102, 15545-15550.

Sullivan, B.M., Juedes, A., Szabo, S.J., von Herrath, M., and Glimcher, L.H. (2003). Antigen-driven effector CD8 T cell function regulated by T-bet. *Proceedings of the National Academy of Sciences* 100, 15818-15823.

Topalian, S.L., Hodi, F.S., Brahmer, J.R., Gettinger, S.N., Smith, D.C., McDermott, D.F., Powderly, J.D., Carvajal, R.D., Sosman, J.A., Atkins, M.B., et al. (2012). Safety, Activity, and Immune Correlates of Anti–PD-1 Antibody in Cancer. *New England Journal of Medicine* 366, 2443-2454.

Ubaid, U., Andrabi, S.B.A., Tripathi, S.K., Dirasantha, O., Kanduri, K., Rautio, S., Gross, C.C., Lehtimäki, S., Bala, K., Tuomisto, J., et al. (2018). Transcriptional Repressor HIC1 Contributes to Suppressive Function of Human Induced Regulatory T Cells. *Cell Reports* 22, 2094-2106.

Utzschneider, D.T., Charmoy, M., Chennupati, V., Pousse, L., Ferreira, D.P., Calderon-Copete, S., Danilo, M., Alfei, F., Hofmann, M., Wieland, D., et al. (2016). T Cell Factor 1-Expressing Memory-like CD8 + T Cells Sustain the Immune Response to Chronic Viral Infections. *Immunity* 45, 415-427.

Wherry, E.J., Teichgräber, V., Becker, T.C., Masopust, D., Kaech, S.M., Antia, R., von Andrian, U.H., and Ahmed, R. (2003). Lineage relationship and protective immunity of memory CD8 T cell subsets. *Nature Immunology* 4, 225-234.

Wickham, H. (2016). ggplot2: Elegant Graphics for Data Analysis (New York: *Springer-Verlag*).

Wu, T., Ji, Y., Moseman, E.A., Xu, H.C., Manglani, M., Kirby, M., Anderson, S.M., Handon, R., Kenyon, E., Elkahloun, A., et al. (2016). The TCF1-Bcl6 axis counteracts type I interferon to repress exhaustion and maintain T cell stemness. *Science Immunology* 1, eaai8593-eaai8593.

Yan, Y., Cao, S., Liu, X., Harrington, S.M., Bindeman, W.E., Adjei, A.A., Jang, J.S., Jen, J., Li, Y., Chanana, P., et al. (2018). CX3CR1 identifies PD-1 therapy–responsive CD8+ T cells that withstand chemotherapy during cancer chemoimmunotherapy. *JCI Insight* 3.

Zajac, A.J., Blattman, J.N., Murali-Krishna, K., Sourdive, D.J., Suresh, M., Altman, J.D., and Ahmed, R. (1998). Viral immune evasion due to persistence of activated T cells without effector function. *J Exp Med* 188, 2205-2213.

Zerbino, D.R., Achuthan, P., Akanni, W., Amode, M R., Barrell, D., Bhai, J., Billis, K., Cummins, C., Gall, A., Girón, C.G., et al. (2018). Ensembl 2018. *Nucleic Acids Research* 46, D754-D761.

Zhang, N. & Bevan, M. (2011). CD8+ T Cells: Foot Soldiers of the Immune System. *Immunity* 35, 161-168.

Zhang, M., Yang, J., Zhou, J., Gao, W., Zhang, Y., Lin, Y., Wang, H., Ruan, Z., and Ni, B. (2019). Prognostic Values of CD38+CD101+PD1+CD8+ T Cells in Pancreatic Cancer. *Immunol Invest.*

Zhou, X., Ramachandran, S., Mann, M. and Popkin, D. (2012). Role of Lymphocytic Choriomeningitis Virus (LCMV) in Understanding Viral Immunology: Past, Present and Future. *Viruses* 4, 2650-2669.

Zhu, M., Janssen, E., Leung, K., and Zhang, W. (2002). Molecular Cloning of a Novel Gene Encoding a Membrane-associated Adaptor Protein (LAX) in Lymphocyte Signaling. *Journal of Biological Chemistry* 277, 46151-46158.

Zhu, Y., Paniccia, A., Schulick, A.C., Chen, W., Koenig, M.R., Byers, J.T., Yao, S., Bevers, S., and Edil, B.H. (2016). Identification of CD112R as a novel checkpoint for human T cells. *The Journal of Experimental Medicine* 213, 167-176.